# Anharmonicity and asymmetry of Landau levels for a disordered two-dimensional electron gas

Stephane Bonifacie, Christophe Chaubet,* Benoit Jouault, and Andre Raymond
*Groupe d'Etude des Semiconducteurs, UMR CNRS 5650, Université Montpellier II, 34095 Montpellier Cedex, France*
(Received 6 May 2005; revised manuscript received 20 June 2006; published 6 December 2006)

We calculate the density of states of a two-dimensional electron gas located at the interface of a strongly disordered GaAlAs/GaAs heterojunction. The disorder potential is created by two delta doped layers. The first layer includes the parent donors which provides the well with electrons and creates a smooth disorder potential. The second layer is doped with either acceptor or donor impurities, and is located inside the well, thus creating a strongly disordered potential. We calculate the density of states in the presence of a magnetic field of arbitrary strength by taking into account all perturbative terms in the fifth Klauder's approximation. We find an anharmonic spectrum, strongly asymmetric, for the Landau level density of states. At low field, the attractive potential creates the well-known band tails or impurity bands. At higher field, we show that impurity bands are also created by repulsive potentials. We discuss the consequences of the anharmonicity and asymmetry on physical properties in the quantum Hall effect regime.

DOI: 10.1103/PhysRevB.74.245303 PACS number(s): 73.43.−f, 73.20.−r

## I. INTRODUCTION

The physical properties of an electron moving in two dimensions under a perpendicular magnetic field have been widely studied both theoretically and experimentally in the last three decades (for a review see Ref. 1). The density of states (DOS) is one of the central quantities in the study of the quantum Hall effect (QHE). The DOS depends on the disorder potential and characterizes each heterostructure. In the last decade, new types of GaAlAs-GaAs heterojunctions have been grown by several groups[2–11] and studied in the QHE regime. These structures incorporate one delta doped layer behind the spacer to provide a two-dimensional (2D) channel with electrons, and another delta doped layer inside the confining well of conducting electrons. This second layer is doped with Si donors or Be acceptors. Extraordinary magnetotransport properties have been found in such heterostrutures: Haug *et al.*[2] observed a shift of the quantum Hall plateaus, depending on the nature of the impurity (donors or acceptors). Unusual optical properties have also been revealed by Buth *et al.*[3] and Bonifacie *et al.*,[4] who performed far infrared absorption experiments. Under high magnetic field conditions and far infrared irradiation, a second cyclotron line appears, the so-called disorder mode,[3] which is observed only for the acceptor-doped structures. Another remarkable phenomenon is the appearance of a set of additional peaks in the cyclotron resonance spectrum, which has been attributed to localized acceptor states.[4]

The DOS of a noninteracting two-dimensional electron gas (2DEG) in the presence of a perpendicular magnetic field is a series of delta peaks centered on the Landau energies. However, in real systems, Landau levels (LL) are broadened by random impurity scattering. Semielliptic[12,13] or Gaussian[14] functions have been proposed to described the LL shape. The first calculation (analytical) of the DOS was carried out by Ando *et al.*[12,13] using the self-consistent Born approximation (SCBA) and treating the perturbative potential as delta functions (short range potential) without taking into account the LL mixing. This resulted in a symmetric semielliptic DOS, whose constant level broadening $\Gamma$ is determined by the zero field electronic mobility. Until 1988, most microscopic theories[15] and calculations of the DOS[12,14,16,17] either considered only one LL, neglecting inter-LL mixing, or took into account only two or three LLs.[18] The LL mixing and the screening was introduced in the work of Xie, Li, and Das Sarma[19] using the SCBA. The resulting DOS showed a smoother and more realistic shape than that obtained by short range impurities. In the 1990s, calculations of the DOS included acoustic phonon scattering[20–22] and electron electron scattering.[23] Finally, a finite background density between LL peaks was predicted in the case of long range scatterers,[24–26] which could explain experimental results.[27–30]

Although the DOS has been widely studied, calculations were performed by taking into account only a few terms in the perturbative series (SCBA approximations), and always yielded a symmetric and harmonic DOS. However, a more precise shape of the DOS is needed to interpret experimental results obtained by Haug *et al.*,[2] Buth *et al.*,[3] and Bonifacie *et al.*[4] Furthermore, the DOS has always been calculated for either a short range or a long range potential and has never been calculated in the case of the types of sample described above, containing both long range and short range scatterers. In the present work we calculate the DOS of a 2DEG in the presence of a strong disorder which is created by two delta doped layers: the first one behind the spacer, and the second one—doped with Si or Be atoms—located inside the confining well of conducting electrons. We show that the anharmonicity and asymmetry explain the shift of the Hall plateaus observed by Haug *et al.* Our calculations consider all terms of the perturbative series in the fifth Klauder approximation,[31] a method already employed by Serre and Ghazali[32] and by Gold *et al.*[33] in the case of zero magnetic field. We extend the work of Kubisa and Zawadski[34] who solved the one impurity problem and demonstrated that repulsive potentials create localized states in the presence of a magnetic field, by the combined effect of the Lorentz force and the electrostatic confinement. These states unlike donors states, disappear at zero magnetic field.

 

We use the Green function formalism and a numerical method proposed earlier by Klauder:[31] the so-called fifth Klauder's approximation (KVA).[31] The KVA was used once by Ando[12] in the case of high magnetic fields to obtain the DOS of the impurity band. More recently it was employed as well by Serre and Ghazali[32] and Gold *et al.*[33] at zero magnetic field, in three- and two-dimensional systems. The most severe limitation of the KVA is that the multiple occupancy corrections are not taken into account. Consequently the width of the impurity band is overestimated, resulting in a Mott density which is too small.[33,35] We do not incorporate in our model the self-energy part due to the electron-electron interaction. Several approximations for this interaction have been discussed in the literature,[13] but following Ref. 33, the self-energy part $\hat{\Sigma}_{ee}$ only produces a rigid energy shift of the DOS. These approximations do not hold at high magnetic field, when the filling factor is close to one and electron-electron interaction strongly increases the Lande $g$-factor. A complete treatment of the screening effects developed by Das Sarma *et al.* would have led here to intractable numerical calculations but would not have changed the features of our results, i.e., the asymmetry and the anharmonicity of the DOS. Lastly, we take into account the LL mixing and calculate the DOS in all the range of magnetic field accessible in experiments: from low magnetic field ($B<0.1$ T) up to very high field ($B>10$ T).

This paper is organized as follows. In the next section, we present our theoretical procedure. We report the results of the calculations in Sec. III and IV. In Sec. III we discuss the case of the reference sample, which has only one impurity layer, while Sec. IV is devoted to the anharmonic and asymmetrical DOS of strongly disordered samples. In Sec. V, we apply this formalism to the transport properties in the QHE regime and demonstrate that the shift of the Hall plateaus is a natural consequence of the asymmetry of the DOS.

## II. FORMULATION OF THE PROBLEM

In this work, we neglect spin degeneracy, assuming electrons to be spinless fermions. The 2D channel is considered as a homogeneous medium with a dielectric constant $\kappa$ and the charge carriers are noninteracting electrons with an effective mass $m^*$ and a charge $e$. The electrons are free in a bidimensional quantum well created by the potential $U(z)$ of the heterojunction (see Fig. 1). An external magnetic field is applied in the $z$ direction. One or two delta layers of impurities are introduced at a given distance from the GaAlAs/GaAs interface. The first doping layer (behind the spacer) has a concentration comparable to the electron concentration. The second layer of impurities, inside the well, creates sharp potential fluctuations either negative (for donors) or positive (for acceptors). Its concentration is one order of magnitude lower than for the first layer.

### A. The single impurity problem

The single impurity problem solved in Ref. 34 is the starting point of our many impurities problem. However, here we diagonalize their Hamiltonian because this procedure leads to more tractable self-consistent calculations of the Green function than the variational method used by Kubisa and Zawadzki.

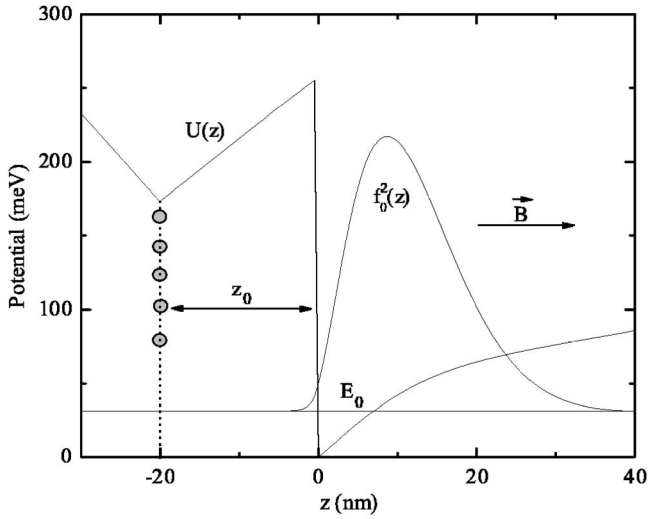


FIG. 1. Schematic view of the heterostructure and the $f_0(z)$ wave function. A delta doped layer is represented here, located at the abscissa $z_0$. A magnetic field is applied along the growth direction.

The impurity located at point $(\mathbf{R}, z_0)$ creates a potential $v_0(\mathbf{r},z)=e^2/[4\pi\kappa\sqrt{(z-z_0)^2+(\mathbf{R}-\mathbf{r})^2}]$. The three-dimensional Hamiltonian of this system is given by

$$\hat{H}=\frac{1}{2m^*}(\hat{\mathbf{p}}+e\hat{\mathbf{A}})^2+\hat{U}+\hat{v}_0, \tag{1}$$

where $\hat{\mathbf{A}}$ is the vector potential operator and $\hat{\mathbf{p}}=(\hat{\mathbf{p}_\perp},\hat{p_z})$ the momentum operator. To solve this equation the three-dimensional problem is first reduced to a bidimensional problem.[36] The wave functions can be approximated by

$$\Psi(x,y,z)=\Phi(x,y)f_0(z), \tag{2}$$

where $f_0(z)$ is the wave function of the first subband of the quantum well with an energy $E_0$:

$$\left(\frac{1}{2m^*}\hat{p}_z^2+\hat{U}\right)f_0=E_0f_0. \tag{3}$$

The eigenenergy $E_0$ is obtained by a variational calculation and $f_0$ is approximated by the modified Fang-Howard trial wave function. Details of this method can be found in Ref. 37. One obtains an effective Schrödinger equation for the $\Phi$ wave function of eigenenergy $E_\perp$:

$$[\hat{H}_\perp+\hat{v}_{\text{bare}}]\Phi=E_\perp\Phi, \tag{4}$$

where

$$\hat{H}_\perp=\frac{1}{2m^*}(\hat{\mathbf{p}}_\perp+e\hat{\mathbf{A}})^2 \tag{5}$$

and

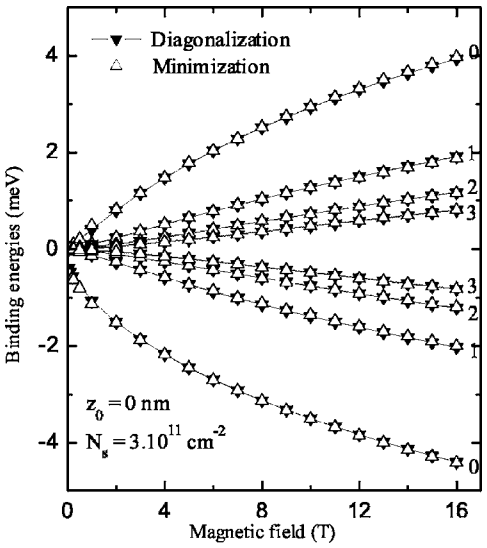


FIG. 2. Binding energies of magnetodonors and magnetoacceptors of the first Landau level. Parameters are given in the text. The angular momentum $m$ is labeled 0,1, 2, and 3. Black down triangles: diagonalization. White up triangles: variational calculation in accordance with Kubisa and Zawadzki. At zero magnetic field, the binding energy vanishes for acceptor states but not for donors: the acceptor states exist only in the presence of a high enough magnetic field.

$$\hat{v}_{\text{bare}}(q) = \frac{1}{\pi q \epsilon(q)} \int_{-\infty}^{\infty} f_0(z)^2 e^{-q|z-z_0|} dz. \tag{6}$$

The screening of the bare potential by free carriers has been taken into account in Refs. 38 and 34 by introducing the dielectric function $\epsilon(q)=1+\frac{e^2}{2\kappa}X_0(q)h(q)$, where $X_0$ is the Linhard function in two dimensions[39] and $h(q)$ is a form factor which is due to the electron-electron interaction in the 2DEG. However, in the presence of a magnetic field, the expression of the dielectric function is quite different from that deduced from the familiar Lindhard function in 2D. This is because the presence of a magnetic field modifies both the energy levels and the wave functions. Nevertheless, we do not focus here on the screening of the bare potential by electrons, instead we keep the dielectric function used by Kubisa and Zawadzki.[34] A complete treatment of the oscillatory screening performed by Xi *et al.* and Das Sarma *et al.*[19] would have lead to intractable calculations. The qualitative effect of the oscillatory screening on the density of states will be discussed in Sec. III.

Now, we apply the diagonalization method to the single impurity problem. We use the basis $|N,m\rangle$, $N \in \{0,1,\ldots,\infty\}$, $m \in \{-N,\ldots,\infty\}$ defined by

$$\langle \mathbf{r}|N,m\rangle = \sqrt{\frac{N!}{2\pi l^2 (N+|m|)!}} e^{(-im\phi - r^2/4l^2)} \times \left(\frac{r^2}{4l^2}\right)^{|m|/2} L_N^{|m|/2}\left(\frac{r^2}{2l^2}\right), \tag{7}$$

where $l=\sqrt{\hbar/eB}$ is the magnetic length and $B$ is the magnetic field. Because of the radial symmetry of the problem, calculation can be performed for each value of $m$ separately. In Fig. 2 we plot the calculated binding energies of magnetodonor and magnetoacceptor states related to the first LL. The impurities are located at the interface ($z_0=0$). The parameters are the same as those used by Kubisa and Zawadzki:[34] for a typical GaAs/AlGaAs heterojunction, the barrier height is 0.257 eV, the effective mass for the AlGaAs barrier and the GaAs well are, respectively, $0.073m_0$ and $0.066m_0$. We took a relative dielectric constant $\kappa_r=12.9$ throughout the entire heterostructure. The electron density and the depletion density have been taken as $N_s=3\times10^{11}$ cm$^{-2}$ and $N_a=6\times10^{10}$ cm$^{-2}$, respectively. The diagonalization has been performed in a basis containing a finite number of LLs. We have included all LLs whose energy is smaller than or comparable to the binding energy $E_b$. At $B=10$ T, 10 LLs were considered to obtain a precision better than 0.1%. At $B=0.1$ T, 150 LLs were considered to obtain a precision of 5%. Figure 2 shows that there is no quantitative difference between the binding energies obtained by our method and those obtained by the minimization procedure of Kubisa and Zawadzki. However, the good convergence of the diagonalization guarantees a reasonable calculation time for the self-consistent procedure, as will be described later.

The second step of the calculation was to fit the true impurity potential by a Gaussian potential defined by

$$v(r) = \frac{V_0}{\pi d^2} \exp\left(-\frac{r^2}{d^2}\right). \tag{8}$$

This potential allowed us to calculate the binding energies more efficiently and therefore to optimize the algorithm used in the second part of this work. $V_0$ is the strength of the potential and $d$ is its spatial extent. In the case $z_0=0$, we obtain a good fit of the binding energies by taking $d=10.4$ nm and $V_0/\pi d^2=22$ meV. Thus we are in the regime of short-range scattering impurities (i.e., following Ref. 13: $d<l/\sqrt{2N+1}$ where $N$ is the LL index) for a wide range of magnetic fields: $0<B<6$ T. If $z_0=500$ Å, the optimized parameters are $d=50$ nm and $V_0/\pi d^2=0.17$ meV. When impurities are close to the electrons, the Gaussian potential is short range, only becoming long range when the impurity layer is far from the electron gas.

### B. The Green function formalism

Now we consider the case of randomly distributed impurities which are all located at a distance $z_0$ of the heterointerface. The Hamiltonian is

$$\hat{H} = \hat{H}_\perp + \hat{V}, \tag{9}$$

with

$$\hat{V} = \sum_i \hat{v}_i \tag{10}$$

and

$$\hat{v}_i = \hat{v}(\mathbf{r} - \mathbf{R_i}, z_0). \tag{11}$$

Here $\mathbf{R}_i$ is the in-plane position of the $i$th impurity.

The single particle Green's function of the averaged Hamiltonian is given by the Dyson equation[40]

$$\langle\langle \hat{G} \rangle\rangle = \frac{1}{E - \hat{H}_\perp - \hat{\Sigma}}, \tag{12}$$

where $\hat{\Sigma}$ is the proper self-energy part that we calculate by means of the KVA and $\langle\langle \cdots \rangle\rangle$ denotes the spatial average. This approximation has been widely used[12,32] although it is known to overestimate the width of the impurity bands.[41] This approximation is performed in two steps. First, one isolates scattering processes $\hat{t}_i$ occurring on a single impurity:

$$\hat{t}_i = \hat{v}_i + \hat{v}_i \hat{P} \hat{v}_i + \cdots, \tag{13}$$

where $\hat{P} = 1/(E - \hat{H}_\perp)$ is the free electron propagator. Then, one sums over all the impurities:

$$\hat{t} = \sum_i \hat{t}_i = \sum_i \hat{v}_i (\hat{1} - \hat{P}\hat{v}_i)^{-1}. \tag{14}$$

Afterwards, $\hat{P}$ is replaced by the dressed propagator $\hat{G}$:

$$\hat{t} = \sum_i \hat{v}_i (\hat{1} - \hat{G}\hat{v}_i)^{-1} \tag{15}$$

and the average value of Eq. (12) $\langle\langle \cdots \rangle\rangle$ is taken over all possible positions of impurities:

$$\hat{\Sigma} = \langle\langle \hat{t} \rangle\rangle = \left\langle\left\langle \sum_i \hat{v}_i (\hat{1} - \hat{G}\hat{v}_i)^{-1} \right\rangle\right\rangle. \tag{16}$$

Figure 3(a) represents Eq. (16) diagrammatically. Figure 3(b) represents Eq. (12). Other diagrams are represented in Figs. 3(c) and 3(d).

To calculate the average, we follow Ando[12] who used two different bases. The first basis $|N,X\rangle$ is used for averaging over the impurities positions. The vectors of the basis are

$$\langle \mathbf{r}|N,X\rangle = \frac{1}{\sqrt{L}} \exp\left( i\frac{xy}{2l^2} - i\frac{Xy}{l^2} \right) \xi_i(x - X), \tag{17}$$

where $L$ is the length of the system, and $l = \sqrt{\hbar/eH}$ the radius of the cyclotron orbit. The functions $\xi_N(x)$ are

$$\xi_N(x) = \sqrt{\frac{1}{2^N N! \sqrt{\pi} l}} \exp\left( -\frac{x^2}{2l^2} \right) H_n(x/l), \tag{18}$$

where $H_n(x)$ is the $n$th Hermite polynomial.

The second basis $|N,m\rangle_{\mathbf{R}_i}$ is centered on the $i$th impurity. This is the most convenient basis for summing the different scattering processes over a given impurity because the impurity potential has the cylindrical symmetry. The vectors of the basis are defined by

$$\langle \mathbf{r}|N,m\rangle_{\mathbf{R}_i} = \langle \mathbf{R_i} - \mathbf{r}|N,m\rangle \exp\left( i\frac{|\mathbf{r} \wedge \mathbf{R_i}|}{2l^2} \right), \tag{19}$$

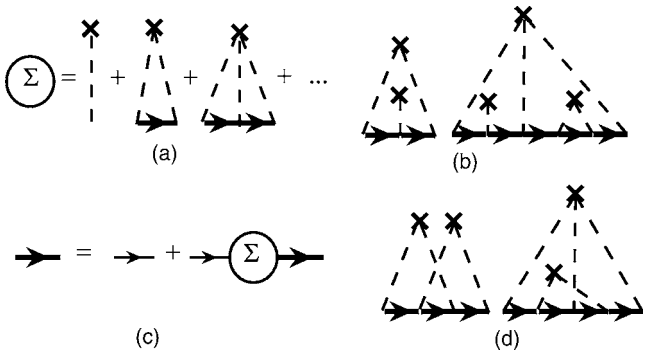


FIG. 3. Electron-impurity diagrams involved in the KVA. (a) Summation of the diagrams of the self-energy; (b) Dyson equation; (c) examples of diagrams that are taken into consideration in the KVA; and (d) examples of diagrams that are neglected. Dashed lines: electron-impurity interaction. Thin full oriented lines: bare propagators. Thick full oriented lines: dressed propagator. Crosses represent impurities.

where the kets $|N,m\rangle$ are defined by Eq. (7). The wave functions of the different bases are linked to each other by the relation

$$|N,X\rangle = \sum_{m=-N}^{\infty} |N,m\rangle_{\mathbf{R}} \sqrt{2\pi l^2} (-1)^m \langle \mathbf{R}|N+m,X\rangle. \tag{20}$$

Finally we assume that

$$\left\langle\left\langle \sum_i |\mathbf{R}_i\rangle\langle \mathbf{R}_i| \right\rangle\right\rangle \simeq N_i. \tag{21}$$

Then, using Eqs. (16), (20), and (21) the self-energy part can be rewritten as

$$\langle N,X|\hat{\Sigma}|N',X'\rangle = 2\pi l^2 N_i \sum_m \langle N,m|\hat{v}(\hat{1} - \hat{G}\hat{v})^{-1}|N,m\rangle \delta_{NN'} \delta_{XX'}. \tag{22}$$

The two main physical parameters appear in Eq. (22). The first one is the dimensionless concentration of impurities, $c = 2\pi l^2 N_i$ which represents the averaged number of impurities seen by one electron. The second parameter is the potential $\hat{v}$. The off-diagonal elements of $\hat{v}$ are responsible for the inter-Landau-Levels mixing (ILLM). We have already mentioned that the potential $\hat{v}$ can be smooth or sharp depending on the location of the doping layer. In the above summation, either the potential is sharp and few values of $m$ are necessary to obtain a good convergence, or the potential is smooth and many values of $m$ are needed. This reflects the spatial extent of the eigenfunctions which need less or more basis elements for their construction.

### C. The density of states

The DOS is directly related to the averaged Green's function by the formula

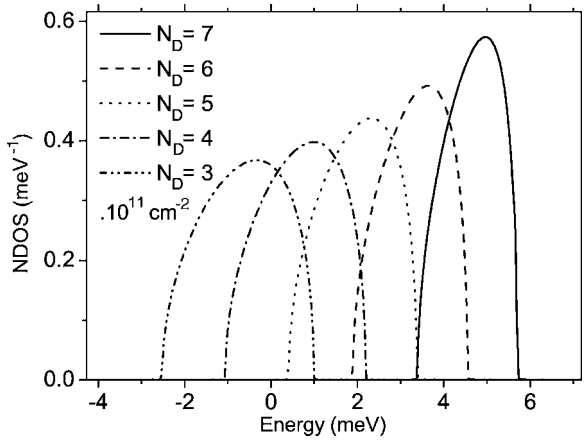


FIG. 4. Density of states at $B=10$ T (ground state) for a GaAlAs/GaAs heterojunction with a Si–$\delta$-doped layer located at 500 Å from the interface. Different curves correspond to different impurity concentration $N_D=(3,4,5,6)\times 10^{11}$ cm$^{-2}$. The surface density is $N_S=3\times 10^{11}$ cm$^{-2}$. More than one-hundred "$m$" have been taken into account.

$$\rho(E) = -\frac{1}{\pi}\,\mathrm{Im}(\mathrm{tr}\langle\langle \hat{G}\rangle\rangle), \tag{23}$$

where $\langle\langle \hat{G}\rangle\rangle$ is calculated from the self-consistent set of Eqs. (12) and (22). The calculation of the DOS consists of summing the matrix (whose rank is the number of LL) indexed by the angular momentum $m$ over all values of the angular momentum $m$, in a self-consistent procedure. In the previous section, the calculation of the binding energies was made by summing over each LL, for each particular value of the angular momentum $m$.

The DOS is represented throughout the paper by its normalized value (NDOS) defined by the relation $NDOS(E)=\rho(E)/(eB/h)$. $NDOS(E)$ verifies

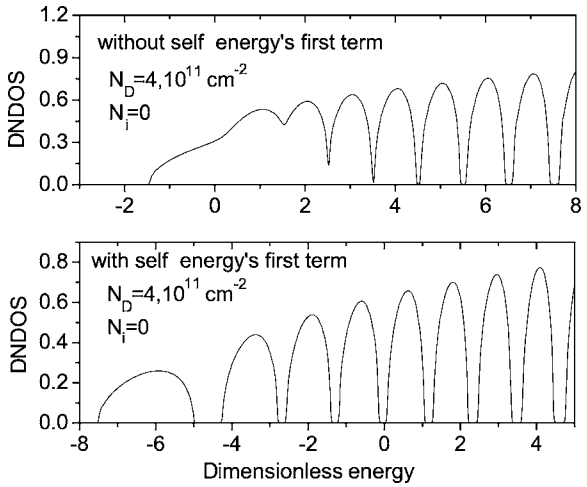


FIG. 5. When the first term of the self-energy is neglected, the Landau ladder is harmonic. When this term is included, the Landau ladder is anharmonic.

$$\int NDOS(E)dE = 1. \tag{24}$$

It is represented as a function of the energy ($E$ in mev and NDOS in mev$^{-1}$) or as a function of the dimensionless energy $\frac{E-\hbar\omega_c}{\hbar\omega_c}$. We use also the dimensionless NDOS, defined by $DNDOS=NDOS\times\hbar\omega_c$.

## III. DENSITY OF STATES IN THE PRESENCE OF A SMOOTH POTENTIAL: REFERENCE SAMPLE

We consider here the reference sample, which has only one $\delta$-doped layer of Si donors in the GaAlAs barrier, at a distance $z_0=-500$ Å from the interface. The disorder potential is smooth. The case of enhanced potential fluctuations by a second layer of impurities (acceptors Be or donors Si) is discussed in the next section.

In this part, we have restricted our attention to the low coupling regime between LLs, when the cyclotron energy $\hbar\omega_c$ is larger than the Landau level broadening $\Gamma$. In this case, each Landau level can be treated separately. Therefore the matrix reduces to a single real number, for each value of the angular momentum $m$. Nevertheless, a large number of $m$ values is necessary to obtain the convergence of the self-consistent calculation. The total number of $m$ necessary to reach the convergence criterium is known when adding a new term changes neither the shape nor the shift of the DOS. Physically this signifies that, to correctly represent the smooth potential, a large number of states $|N,m\rangle$ are required.

Figure 4 represents the general shape of the ground state Landau level whose width is overestimated by our method. There are two main differences between this shape compared with the elliptic shape obtained by Ando[12,13,18] or the Gaussian shape obtained by Brezin *et al.*[14] First, the asymmetry of the DOS is enlarged on its low energy side because of the donor character of impurities. Second, there is a global shift of the DOS towards the low energy side. This shift is due to the first term in the calculation of the self-energy. This first term, which represents the mean potential seen by one electron, is generally not taken into account. The shift is a decreasing function of the LL index, as illustrated in Fig. 5 and results in an anharmonicity of the Landau ladder. We stress that this effect should be experimentally confirmed by magnetophotoluminescence experiments in the low magnetic field range.[42] Taking into account the screening would induce a $1/B$ oscillatory behavior of the Landau levels width, and of the LL anharmonicity. For an even filling factor, when the Fermi level lies between 2 LLs, the screening would be negligible and the anharmonicity would be maximum, whereas for an odd filling factor (when the Fermi level lies in the middle of a LL), the screening would be maximum and the anharmonicity minimum.[19]

Finally, we present in Fig. 6 the DOS of the first two LLs for different magnetic field values on a dimensionless scale. We observe the suppression of the shift when the magnetic field is increased. The energies of the perturbed LLs are clearly approaching the unperturbed energies at high magnetic field: the ladder is now harmonic.

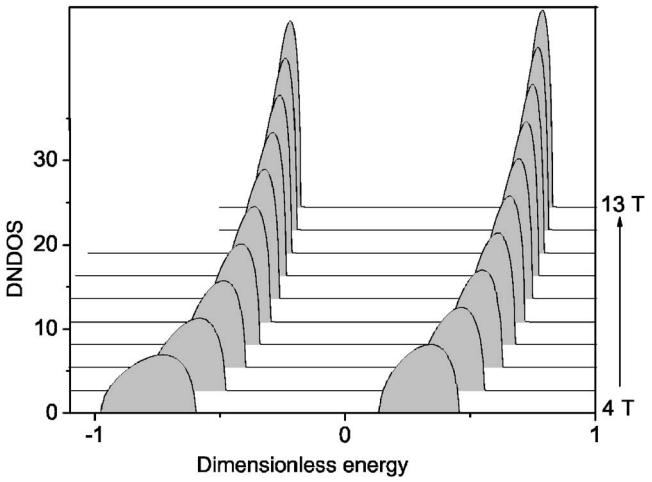


FIG. 6. Density of states for GaAlAs/GaAs heterojunctions with only one Si-doped delta layer located at 500 Å from the interface, for different magnetic fields. The abscissa axis is shifted by $\frac{\hbar\omega_c}{2}$ and normalized by $\hbar\omega_c$. The vertical axis is normalized by $\frac{eB}{h}/\hbar\omega_c$, and curves are shifted for clarity.

## IV. DENSITY OF STATES IN THE PRESENCE OF BOTH SMOOTH AND SHARP POTENTIALS

### A. High magnetic field

In the presence of high magnetic field, ILLM can be neglected because the dimensionless impurity concentration is small ($c=4\times10^{-2}$ for $N_i=1.10^{10}$ cm$^{-2}$ at $B=10$ T). The localized states shrinks with increasing $B$, thus the overlap integral between two different impurities becomes negligible. Each impurity can be considered as isolated from each other and the calculations tend to the case of one impurity treated in Ref. 34.

The density of states in the high field limit is represented in Figs. 7(a) and 7(b), respectively, for donors and acceptors. We observe the formation of impurity bands (IBs) on the low energy side in the case of donors, and on the upper energy side for acceptors. The energy ranges of IBs are certainly overestimated due to the method used to treat the disorder. However, we can observe that each isolated band appearing at low density, which corresponds to levels of different angular momentum ($m=0,1,2,3,\ldots$), is exactly centered on the binding energy calculated by Kubisa and Zawadzki.[34] Counting the total number of states of an impurity band which is entirely separated from the LL, one obtains the impurity density $N_i$. If $E_{B1}$ ($E_{B2}$) represents the lower (higher) band edge of the IB, then, neglecting the spin degeneracy:

$$\int_{E_{B1}}^{E_{B2}} \rho(E)dE = 2N_i.$$

We observe the formation of an impurity band for densities $N_i \leqslant 2.10^{10}$ cm$^{-2}$. When the impurity concentration increases, the bandwidth increases as well until overlapping at a critical density $N_{ic}=2.10^{10}$ cm$^{-2}$ at $B=10$ T in our case. More precisely, this critical density depends on several parameters:

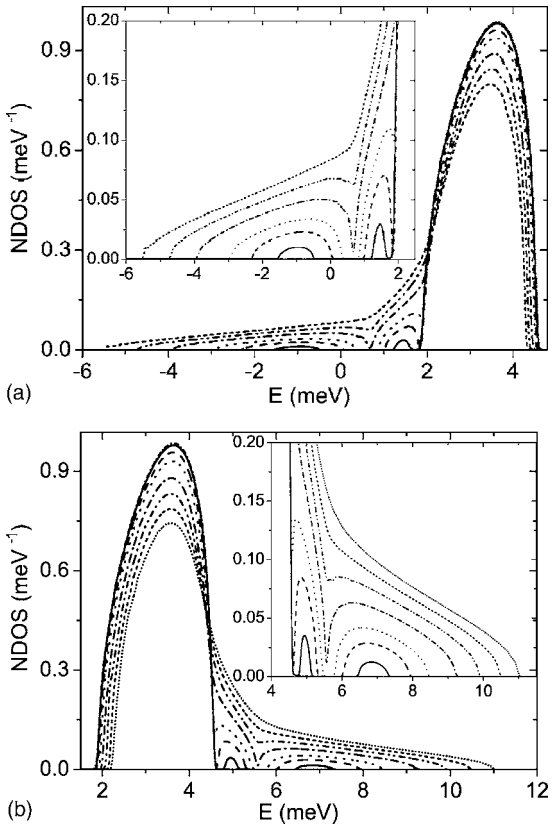


FIG. 7. Influence of the doping density on the normalized density of states at $B=10$ T for the first LL, in the case of a GaAlAs/GaAs heterojunction having two delta-doped layers. First delta-doped layer: concentration $N_D=4.10^{11}$ cm$^{-2}$ of Si-atoms at $z_0=500$ Å. Second doping layer: Si atoms (curve a) or Be atoms (curve b) at $z_0=0$. Different curves correspond to different density of the second layer: $N_i=0;0.1;0.5;1;2;3;4;5\times10^{10}$ cm$^{-2}$.

the position of the doping layer, the 2D electron density $N_S$, and the magnetic field $B$.

In Fig. 8, we show the normalized density of states for several values of the magnetic field. The two sets of curves correspond to the acceptor and donor case. We notice that the global shift represented in Fig. 6 is not strongly modified by the additional low-density impurity layers (Fig. 8). Increasing the magnetic field strength then leads to the formation of a separated impurity band for the $N=0$ LL. At low field, this impurity band collapses to form a band tail. For the first excited LL, no separated impurity band is created because the binding energies are too small.

### B. Intermediate magnetic field

The DOS is calculated for $B=0.5$ T and different impurities concentrations. We represent the case of donors in Fig. 9 and the case of acceptors in Fig. 10. The condition $c=1$ is obtained for $N_i=1.2\times10^{10}$ cm$^{-2}$. In both cases the DOS is enlarged in the low energy side by the long range potential fluctuations of attractive Si parents donors at 500 Å from the interface. The additional short range potential fluctuations at the interface modify the DOS: attractive Si impurities enlarge the DOS on the same side as the parent donors,

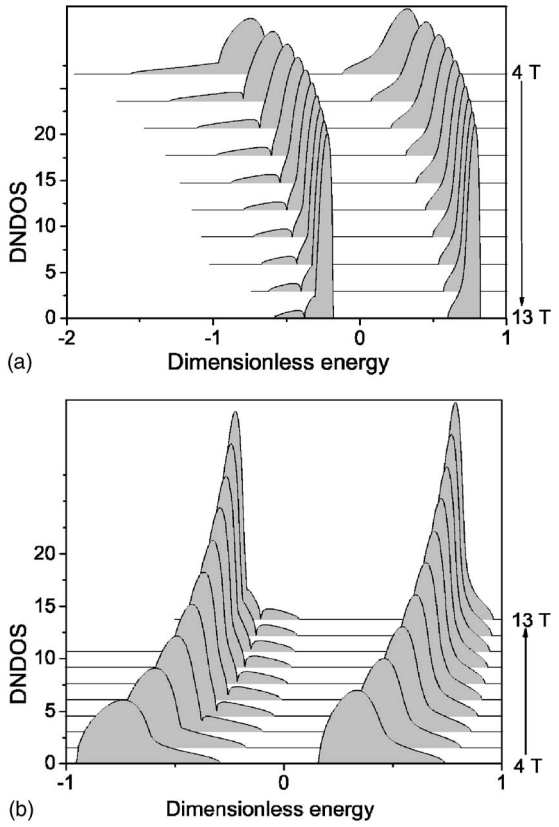


FIG. 8. Density of states for different magnetic field values, in the case of a GaAlAs/GaAs heterojunction having two delta-doped layers. First delta layer: Si atoms at $z_0=500$ Å. Second doping layer: (a) Si atoms at $z_0=0$ and (b) Be atoms at $z_0=0$. The abscissa axis is shifted by $\frac{\hbar\omega_c}{2}$ and normalized by $\hbar\omega_c$. The vertical axis is normalized by $\frac{eB}{h}/\hbar\omega_c$, and curves are shifted for clarity.

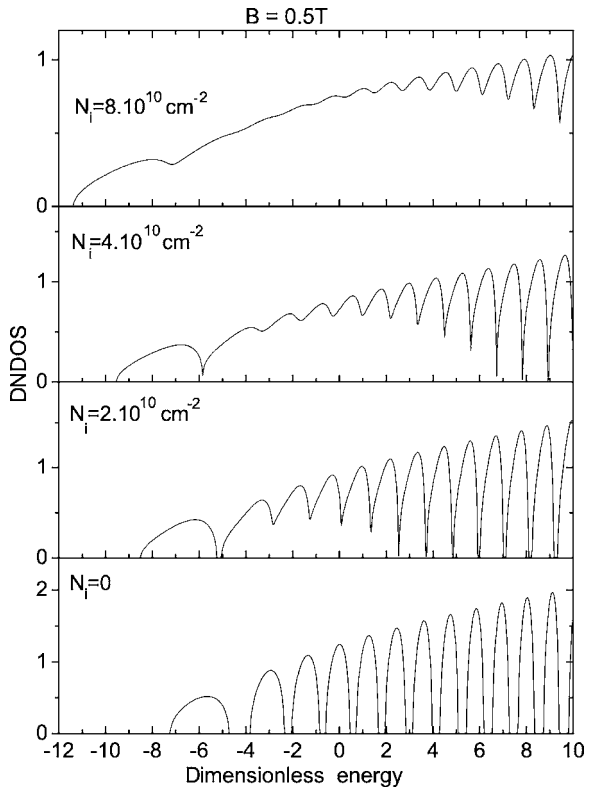


FIG. 9. Density of states in the presence of donors, for GaAlAs/GaAs heterojunctions having a delta layer of Si at 500 Å from the interface, and another delta layer (density $N_i$) of Si located at the interface. The magnetic field is $B=0.5$ T. The critical density is $N_i=1.2\times10^{10}\text{cm}^{-2}$.

whereas Be impurities enlarge the DOS on the other side.

Up to the critical value $c=1$, the degeneracy of the first LL is large enough to contain all impurities states. When the density of the impurity layer increases ($c\geqslant1$), the LLs overlap as shown in Fig. 9. The first LL remains separated from the higher LLs for a wider range of concentration values because the shift is more important for low LL index $N$, as previously mentioned.

Figure 10 is dedicated to the acceptor case. Now, the first LL remains separated from the Landau ladder even at the higher density of $N_i=8.10^{-10}$ cm$^{-2}$ and the merging of LLs begins by the high values of $N$. This difference between acceptors and donors is related to the difference which is observed at $B=0$ T: i.e., only donors states exist at very low $B$.

### C. Low magnetic field

Figure 11 shows the DOS in the case of donors impurities at $B=0.1$ T. Different values of the donor concentration $N_i$ have been considered, and the energy shift between different curves has been removed. The energy reference is fixed at the center of the first unperturbed Landau level. The high energy side of some curves has been cut off for clarity. In the acceptor case, which is not represented here, no IB below the conduction band appear.

At low field, ILLM becomes dominant: LLs overlap and tend to the flat conduction band (CB) of a 2DEG at $B=0$ T. At such a low $B$, the degeneracy of one LL is smaller than $2N_i$ and several LLs contribute to the formation of the IB (ILLM). Figure 11 represents the donor case. In agreement with Fig. 2, only one IB exists, corresponding to $m=0$.

The critical density ($c=1$) is represented by trace 7 in Fig. 11. Above $c=1$, the IB and the CB merge and form a band tail. At vanishing concentration $c$, the position of the IB is again in perfect agreement with the binding energies calculated in Sec. II (see Fig. 2).

These results are in good agreement with the theoretical results of Gold, Serre, and Ghazali[33] who calculated the DOS of a 2DEG in the case $B=0$ T within the same Klauder's approximation.

We do not observe the formation of a second IB that could originate from states of higher momenta. It should be noted that our potential does not allow the formation of excited impurity bands at vanishing magnetic field because all the binding energies vanish at $B=0$ T, except for $m=0$. The disappearance of the IB occurs at a concentration $N_i^c=0.5\times10^{10}$ cm$^{-2}$. Gold *et al.* pointed out that the enhanced Thomas-Fermi screening they used implied large impurity bandwidth. However, the critical metal-insulator densities we found are so small that they are more probably related to the errors induced by the Klauder V approximation itself.[35]

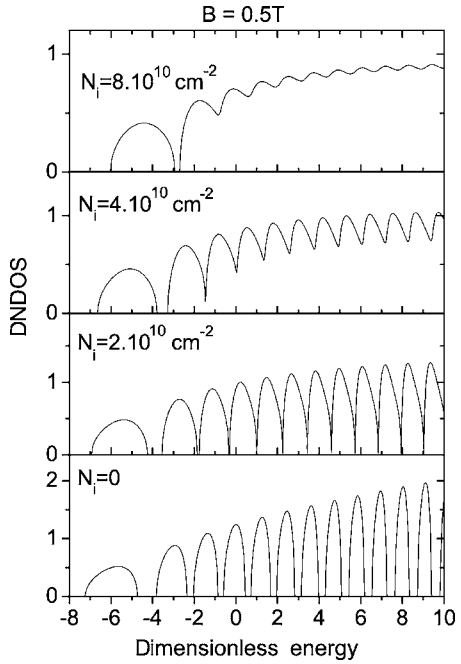


FIG. 10. Density of states in presence of acceptors, for a GaAlAs/GaAs heterojunctions having a delta layer of Si at 500 Å from the interface, and another delta layer (density $N_i$) of Be located at the interface. The magnetic field is B=0.5 T.

## V. QUANTUM HALL EFFECT

It has been established in GaAs/GaAlAs heterostructures that a 2DEG perturbed by acceptor or donor impurities exhibits shifts of the quantum Hall plateaus relative to the line for the classical Hall resistance.[2] If acceptors (donors) are added, then the plateaus shift to lower (higher) filling factor $\nu$. These shifts are successfully explained by the asymmetry of the DOS in each LL. Because our theoretical approach takes into account ILLM, the Hall resistivity $R_H$ at both high and low magnetic fields can be calculated and therefore a direct comparison between the classical Hall effect and the shifts of the plateaus is possible.

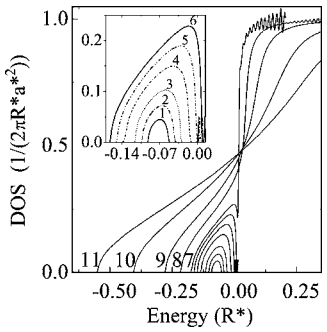


FIG. 11. The density of states at $B$=0.1 T in the case of magnetodonors, and for different impurity concentrations. The curves labeled from 1 to 11 correspond to concentrations 0.01, 0.025, 0.05, 0.1, 0.15, 0.2, 0.25, 0.5, 1, 2.5, and $5.0\times10^{10}$ cm$^{-2}$, respectively. Curve 7 corresponds to the concentration $N_i=0.25\times10^{10}$ cm$^{-2}$ for which $c=1$. Inset: enlargement of the IB at low donor concentrations. The flat conduction band degeneracy is equal to $\frac{m}{\pi\hbar^2}$.

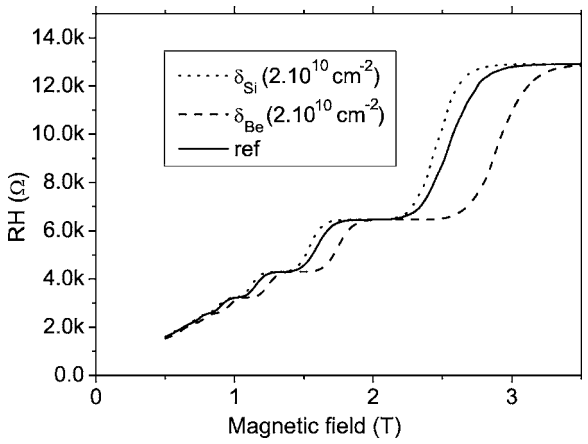


FIG. 12. Three curves corresponding to three different "samples." Reference is represented by a full line. The Hall resistance of the acceptor-doped sample is shifted towards low filling factors (higher $B$), whereas it is shifted towards high filling factors (lower $B$) in the case of donors.

For simplicity we assume that only one state per LL is delocalized whose energy $E_n$ is given by the maximum of the $n$th LL.[43] Furthermore, we assume that this state exists even in the presence of strong disorder and ILLM, and its contribution to the conductivity is $e/h$. Within these approximations, the adiabatic conductivity is given by

$$R_H^{-1} = \frac{e^2}{h}\sum_n f(E_F - E_n), \tag{25}$$

where $f$ is the Fermi distribution and $E_F$ is the Fermi energy. Figure 12 shows the calculated Hall resistance as a function of the magnetic field $B$. For all of the three cases of Fig. 12 a $\delta$-doped layer located at 500 Å from the interface, with a concentration $N_D=4.10^{11}$ cm$^{-2}$, contains the parent donors. A second $\delta$ layer of donors (acceptors) is added at $z_0=0$, and shifts the curve towards low (high) magnetic fields, compared to the reference case. The figure reproduces well the shift of the Hall plateaus, and must be compared to Figs. 1 and Fig. 2 of Ref. 2. Experimentally, the shift of the plateaus is always much less pronounced for donors than for acceptors, and this effect is reproduced here. The reason for this lies in the fact that the remote layer is always doped with donors. At low field the three curves of Fig. 12 merge into the same classical line.

## VI. CONCLUSION

We have used the multiple scattering approach proposed by Klauder and the averaging procedure proposed by Ando to calculate the density of states of a strongly disordered two-dimensional electron gas under a magnetic field of arbitrary strength. We have considered all terms in the perturbative series. One observes, even in presence of a smooth disorder, a strong anharmonicity of the Landau ladder due to the first term in the calculation of the self-energy.

When we analyze the situation of a strong disorder potential, we must consider two cases: At low field, for strong attractive disorder potential (donor impurities), the density of states exhibits either an impurity band or a band tail, depending on the impurity concentration. In the case of a strong repulsive disorder potential (acceptor impurities), there is neither impurity band nor band tail. At higher field, one observes for both cases that impurity bands split from the free Landau level states: the situation for attractive and repulsive disorder potential becomes symmetric at high fields when the mixing between the Landau levels can be neglected.

Our results are in good qualitative agreement with an experimental study of the metal-nonmetal transition in GaAs-GaAlAs heterostructures,[44] with recent magnetophotoluminescence experiments[45] and transport experiments[2] in the Quantum Hall regime.

## ACKNOWLEDGMENT

We are grateful to B. Etienne and W. Zawadzki for helpful discussions.

*Author to whom correspondence should be addressed. Email address: chaubet@ges.univ-montp2.fr

[1] *The Quantum Hall Effect*, edited by R. E. Prange and M. Girvin (Springer-Verlag, New York, 1987).
[2] R. J. Haug, R. R. Gerhardts, K. v. Klitzing, and K. Ploog, Phys. Rev. Lett. **59**, 1349 (1987).
[3] K. Buth, M. Widmann, A. Thieme, and U. Merkt, Semicond. Sci. Technol. **18**, 434 (2003); U. Merkt, Phys. Rev. Lett. **76**, 1134 (1996); M. Widmann, U. Merkt, M. Cortes, W. Haussler, and K. Eberl, Physica B **249**, 762 (1998).
[4] S. Bonifacie, Y. M. Meziani, S. Juillaguet, C. Chaubet, A. Raymond, W. Zawadzki, V. Thierry-Mieg, and J. Zeman, Phys. Rev. B **68**, 165330 (2003).
[5] H. P. van der Meulen, D. Sarkar, J. M. Calleja, R. Hey, K. J. Friedland, and K. Ploog, Phys. Rev. B **70**, 155314 (2004).
[6] Q. X. Zhao, S. Wongmanerod, M. Willander, P. O. Holtz, S. M. Wang, and M. Sadeghi, Phys. Rev. B **63**, 195317 (2001).
[7] M. P. Halsall, P. Harrison, J.-P. R. Wells, I. V. Bradley, and H. Pellemans, Phys. Rev. B **63**, 155314 (2001).
[8] S. Wongmanerod, B. Sernelius, P. O. Holtz, B. Monemar, O. Mauritz, K. Reginski, and M. Bugajski, Phys. Rev. B **61**, 2794 (2000).
[9] P. O. Holtz, A. C. Ferreira, B. E. Sernelius, A. Buyanov, B. Monemar, O. Mauritz, U. Ekenberg, M. Sundaram, K. Campman, J. L. Merz, and A. C. Gossard, Phys. Rev. B **58**, 4624 (1998).
[10] M. Hayne, A. Usher, A. S. Plaut, and K. Ploog, Phys. Rev. B **50**, 17208 (1994).
[11] I. V. Kukushkin, R. J. Haug, K. vonKlitzing, K. Eberl, and K. Totemeyer, Phys. Rev. B **50**, 11259 (1994).
[12] T. Ando and Y. Uemura, J. Phys. Soc. Jpn. **36**, 959 (1974); T. Ando, *ibid.* **36**, 1521 (1974).
[13] T. Ando, A. B. Fowler, and F. Stern, Rev. Mod. Phys. **54**, 437 (1982).
[14] E. Brezin, D. J. Gross, and C. Itzykson, Nucl. Phys. B **235**, 24 (1984).
[15] R. Joynt and R. E. Prange, Phys. Rev. B **29**, 3303 (1984); G. F. Giuliani, J. J. Quinn, and S. C. Ying, *ibid.* **28**, 2969 (1983); B. I. Halperin, *ibid.* **25**, 2185 (1982); D. J. Thouless, J. Phys. C **14**, 3475 (1981).
[16] F. Wegner, Z. Phys. B: Condens. Matter **51**, 279 (1983).
[17] I. Affleck, J. Phys. C **16**, 5839 (1983).
[18] T. Ando, J. Phys. Soc. Jpn. **52**, 1740 (1983); **53**, 3101 (1984); **53**, 3126 (1984).
[19] S. Das Sarma and X. C. Xie, Phys. Rev. Lett. **61**, 738 (1988); X. C. Xie, Q. P. Li, and S. Das Sarma, Phys. Rev. B **42**, 7132 (1990).
[20] N. Mori, H. Murata, K. Taniguchi, and C. Hamaguchi, Phys. Rev. B **38**, 7622 (1988).
[21] B. Tanatar, M. Singh, and A. H. MacDonald, Phys. Rev. B **43**, 4308 (1991).
[22] W. Xu and P. Vasilopoulos, Phys. Rev. B **51**, 1694 (1995).
[23] A. L. Efros, F. G. Pikus, and V. G. Burnett, Solid State Commun. **84**, 91 (1992).
[24] L. Spies, W. Apel, and B. Kramer, Phys. Rev. B **55**, 4057 (1997).
[25] V. Sa-yakanit, N. Choosiri, and H. R. Glyde, Phys. Rev. B **38**, 1340 (1988).
[26] K. Broderix, N. Heldt, and H. Leschke, Phys. Rev. B **40**, 7479 (1989).
[27] R. Lassnig and E. Gornik, Solid State Commun. **47**, 959 (1983).
[28] J. P. Eisenstein, H. L. Stormer, V. Narayanamurti, A. Y. Cho, A. C. Gossard, and C. W. Tu, Phys. Rev. Lett. **55**, 875 (1985).
[29] E. Gornik, R. Lassnig, G. Strasser, H. L. Stormer, A. C. Gossard, and W. Wiegmann, Phys. Rev. Lett. **54**, 1820 (1985).
[30] D. Heitmann, M. Ziesmann, and L. L. Chang, Phys. Rev. B **34**, 7463 (1986).
[31] J. R. Klauder, Ann. Phys. (N.Y.) **14**, 43 (1961).
[32] J. Serre and A. Ghazali, Phys. Rev. B **28**, 4704 (1983).
[33] A. Gold, J. Serre, and A. Ghazali, Phys. Rev. B **37**, 4589 (1988).
[34] M. Kubisa and W. Zawadzki, Semicond. Sci. Technol. **11**, 1263 (1996).
[35] J. Monecke, J. Kortus, and W. Cordts, Phys. Rev. B **47**, 9377 (1993).
[36] J. A. Brum, G. Bastard, and C. Guillemot, Phys. Rev. B **30**, 905 (1984).
[37] G. Bastard, *Wave Mechanics Applied to Semiconductor Heterostructures* (Editions de Physique, Les Ulis, 1988).
[38] J. Price, J. Vac. Sci. Technol. **19**, 599 (1981).
[39] F. Stern, Phys. Rev. Lett. **18**, 546 (1967).
[40] A. L. Fetter and J. D. Walecka, *Quantum Theory of Many-Particle Systems* (McGraw-Hill, New York, 1971).
[41] R. J. Elliot, J. A. Krumhansl, and P. L. Leath, Rev. Mod. Phys. **46**, 465 (1974).
[42] The magnetophotoluminescence experiments are usually performed at high magnetic field, whereas the anharmonicity is enhanced at low values of the magnetic field. This can explain why this effect has not yet been experimentally evidenced. Indeed, the first term of the expansion series represents the mean potential seen by one electron. Then, at low magnetic field, one

electron sees many impurities because of the large value of its magnetic length. This results in a larger mean potential value and a stronger anharmonic effect. When the field is increased, the magnetic length decreases as $1/\sqrt{B}$ and the mean potential seen by one electron decreases as $1/B$, which reduces the anharmonicty.

[43] R. B. Laughlin, Phys. Rev. B **23**, 5632 (1981).

[44] J. L. Robert, A. Raymond, L. Konczewicz, C. Bousquet, W. Zawadzki, F. Alexandre, I. M. Masson, J. P. Andre, and P. M. Frijlink, Phys. Rev. B **33**, 5935 (1986).

[45] P. Vicente, A. Raymond, M. Kamal Saadi, R. Couzinet, M. Kubisa, W. Wawadzki, and B. Etienne, Solid State Commun. **96**, 90 (1995).